

1 *Article*
2 **EFFECTS OF LIGHT DOSIMETRY IN PHOTOBLEACHING OF THE**
3 **PHOTOSENSITIZER (PS) AND CYANINE DYE (CD) MOIETIES IN PS-CD**
4 **CONJUGATES AND ITS CORRELATION WITH PHOTODYNAMIC**
5 **THERAPY (PDT) EFFICACY**

6 **Nadine James**¹, **Ravindra R. Cheruku**¹, **Joseph R. Missert**¹, **Ulas Sunar**^{1,2}, and **Ravindra K**
7 **Pandey**^{1,*}

8 ¹ PDT Center, Cell Stress Biology, Roswell Park Cancer Institute, Buffalo, NY 14263

9 ² Department of Biomedical Engineering, Wright State University, Dayton, OH 45435

10 * Correspondence: ravindra.pandey@roswellpark.org; Tel.: 716-845-3203

11

12

13 **Abstract:** Photodynamic therapy (PDT) of cancer is dependent on three primary components:
14 photosensitizer (PS), light, and oxygen. Because these components are interdependent and vary
15 during the dynamic process of PDT, assessing PDT efficacy may not be trivial. Therefore, it has
16 become necessary to develop pre-treatment planning, on-line monitoring and dosimetry strategies
17 during PDT, which become more critical for two or more chromophore systems, e.g. PS-CD
18 conjugates developed in our laboratory for fluorescence-imaging and PDT of cancer.

19 In this study, we observed a significant impact of variable light dosimetry; (i) high light fluence and
20 fluence rate (light dose: 135 J/cm², fluence rate: 75 mW/cm²) and (ii) low light fluence and fluence
21 rate (128 J/cm² and 14 mW/cm² and 128 J/cm² and 7 mW/cm²) in photobleaching of the individual
22 chromophores and their long-term tumor response. The fluorescence at the near-infrared (NIR)
23 region of the PS-NIR fluorophore conjugate was assessed intermittently via fluorescence imaging.
24 The loss of fluorescence, photobleaching, caused by singlet oxygen from the PS was mapped
25 continuously during PDT. The tumor responses (BALB/c mice bearing Colon26 tumors) were
26 assessed after PDT by measuring tumor sizes daily. Our results showed distinctive photobleaching
27 kinetics rates between the PS and CD. Interestingly, compared to higher light fluence, the tumors
28 exposed at low light fluence showed reduced photobleaching and enhanced long-term PDT
29 efficacy. The presence of NIR fluorophore in PS-CD conjugates provides an opportunity of
30 fluorescence imaging and monitoring the photobleaching rate of the CD moiety for large and
31 deeply seated tumors and assessing PDT tumor response in real-time.

32 **Keywords:** Photodynamic therapy, photobleaching, photosensitizers, fluorescence imaging.

33

34 **1. Introduction**

35 PDT was initially developed for the local destruction of solid tumors [1, 2] and is currently being
36 used worldwide in the treatment of several tumors including skin basal cell carcinoma (BCC) [3],
37 lung [4-6], esophagus [7-11], bladder, head and neck [4,6,12], brain [13-17], ocular melanoma,
38 ovarian, prostate [8-20], renal cell, cervix, pancreas and bone [21]. It is also being used for a plethora
39 of additional indications such as, dysplasia, papillomas, rheumatoid arthritis, age related macular
40 degeneration, actinic keratosis, cosmesis, psoriasis, endometrial ablation, localized infection
41 (bacterial and fungal) and prophylaxis of arterial restenosis. Considering that the use of PDT has
42 been approved for many diseases, it is still not being practiced in mainstream oncology. The
43 partial reason for this is that the treatment outcome cannot be foreseen clearly, as the therapy
44 related dosimetry based on measured or calculated physical values is not yet optimized.

45 PDT is known to be dependent on three primary components: Photosensitizer (PS), light, and
46 oxygen in order to deliver an effective dose¹. Therefore, it is necessary to establish an
47 understanding of the basic physical and biophysical interactions of these three essential
48 components to maximize PDT output. Over the past two decades, much work has been done to
49 optimize these components, but their dynamic nature and complex interdependency lead to
50 complexity. Therefore, to understand the PDT dosimetry, which is intended to quantify a
51 therapeutic outcome, is of importance to provide reliable tool for controlled enhancement of the
52 PDT outcome.

53 Currently most of the photosensitizers (PSs) used in PDT elicit significant damage to cancer cells
54 through singlet oxygen mediated pathways [1]. The standard approach in clinical PDT is to use
55 the prescribed treatments that involve using fixed amounts of photosensitizer (per unit body
56 weight), incident light fluence (J/cm²) and fluence rates (total energy delivered within a specific
57 drug-light time interval (mW/cm²)) [22] to treat each patient. However, this sometimes leads to
58 incomplete or unpredictable responses in patient groups, which may be due to differences in
59 individual physiological effects [22,23]. These heterogeneous factors include local tissue optical
60 properties, tumor oxygenation and accumulated photosensitizer dose, which can be very different
61 for each patient and tumor. These factors also may change differently during PDT. For example,
62 photobleaching of the PS may reduce singlet oxygen production which may cause ground-state
63 oxygen to be depleted if the reperfusion capacity of the tissue is exceeded by the immediate
64 photochemical reaction [24]. Therefore, it has become necessary to develop pretreatment planning,
65 on-line monitoring and dosimetry strategies during PDT [1].

66 Optimization of clinical dosimetry methods can follow one of three paths as described previously
67 (see for example McIlroy *et al* [24], Wilson *et al* [25] and Zhu [26]) and can be classified as direct [26],
68 explicit or implicit dosimetry [22,25]. Direct dosimetry involves the measurement of singlet oxygen
69 itself, either through emission of its phosphorescence or through singlet oxygen sensitive
70 chromophores [26]. Explicit dosimetry employs techniques and instrumentation to measure the
71 three essential components of photodynamic therapy (light, photosensitizer (PS), and oxygen)
72 individually and independently in the tissue [22,25]. A predictive model of the photobiological
73 effect of these three components is required to combine the measurements into a dose metric
74 [22,23,25]. Significant progress has been made in regards to the application of explicit dosimetry
75 but there are still limitations [25]. Implicit dosimetry seeks to avoid measuring the light, PS and
76 oxygen independently by eliciting the use of a single parameter that incorporates two or more of
77 the essential components into a single metric in order to predict the biological damage [1,22,25,27].
78 This is chiefly accomplished by monitoring the PS photobleaching during irradiation by utilizing
79 the fluorescence properties of the PS [22,25].

80 We are engaged in the exploration of PDT dosimetry strategies by employing the implicit
81 dosimetry approach. In our strategy, we aim to investigate the utility of the photosensitizer-near
82 infrared fluorophores conjugate (PS-NIRF) as fluorescence probes and markers for PDT light
83 dosimetry. We hypothesize that the photobleaching characteristics of the fluorophores when
84 subjected to variable light fluence and fluence rates will provide a metric to optimize the light
85 dosimetry and PDT response.

86 If singlet oxygen is the main cytotoxic agent and the main cause of photobleaching, monitoring the
87 photobleaching could provide a quantifiable measure of the singlet oxygen production. Therefore,
88 we monitored the photobleaching of the photosensitizer and the fluorophore within several
89 bifunctional photosensitizer-fluorophore conjugates using real time *in vivo* fluorescence imaging.
90 In our initial attempt, the fluorescence of the NIR fluorophore portion of the conjugate was
91 measured intermittently throughout the PDT treatment. First, *in vitro* photobleaching experiments
92 were performed as a model of the *in vivo* systems to see if they could predict the *in vivo* response.
93 Then, we imaged mice before and after PDT treatment at three different light doses, after exciting

94 the PS or the NIRF portion of the conjugate individually, and investigated potential direct
 95 correlation between photobleaching and PDT efficacy.
 96

97 2. Results and Discussion

98 The degradation of the conjugates was observed via UV-Vis spectroscopy *in vitro*. Although these
 99 solutions of conjugates were made up as 5 μM solutions in 17% Bovine Calf Serum (BCS) it was
 100 understood that the intent was not to reproduce exact solvent conditions used clinically but to
 101 show whether drug aggregation or binding with serum affected the photobleaching of the
 102 chromophores. However, in our *in vivo* photobleaching experiments the degradation of the NIR
 103 fluorophore (CD) portion of the PS-CD conjugates was observed. In later experiments, we observed
 104 the degradation of both PS and CD via fluorescence quenching.
 105

106 2.1. Mechanism of Photo-induced Bleaching

107
 108 Using the NIR CD as a guide, **Figure 1**, illustrates the mechanism of photo-degradation caused
 109 by the contribution of molecular oxygen and light. Interaction of singlet oxygen with the
 110 chromophores constitutes the major pathway of photodecomposition. When the PS (HPPH)
 111 portion of the PS-NIR fluorophore (CD) conjugate absorbs light it undergoes intersystem crossing
 112 from an excited singlet state to an excited triplet state where it interacts with endogenous ground
 113 state triplet oxygen to generate the destructive singlet oxygen species. In the illustration below, the
 114 singlet oxygen generated subsequently attacks the polymethine chain of cypate resulting in
 115 fragmentation of the CD moiety as shown in **Figure 1**.
 116

117 The photoproduct obtained after
 118 photo-induced bleaching is due to
 119 oxidation of the C'- C2 or C7'- C2'' bond
 120 on the polymethine chain. Singlet
 121 oxygen is directed towards the
 122 polymethine chain at the C'- C2 or C7'-
 123 C2'' bond due the electro-positivity of the
 124 2 and 2'' carbon versus the electron rich
 125 position 1' or 7' of the cationic
 126 chromophore [28]. This degradation
 127 generates the corresponding carbonyl
 128 photoproducts [28].

129 2.2. *In Vitro* Photobleaching of HPPH 130 Cyanine Dye and CD Conjugates

131 The conjugates; HPPH-CD (8),
 132 HPPH2CD (9), HPPH-Cypate (10) and
 133 HPPH2-Cypate (11) shown in **Figure 2**
 134 were prepared by following our own
 135 methodology were formulated in 17%
 136 Bovine Calf Serum/PBS and were used
 137 equimolar concentrations (5 μM) for the
 138 studies presented herein [29, 30]. The absorption spectra were measured in 1 cm-quartz cuvettes
 139 following irradiation at 665 nm at various time points until there was complete degradation of the
 140 NIRF portion of the conjugate, **Figure 3**. The photobleaching rates were different, and were in the
 141 following order $9 > 10 > 8 > 11$.

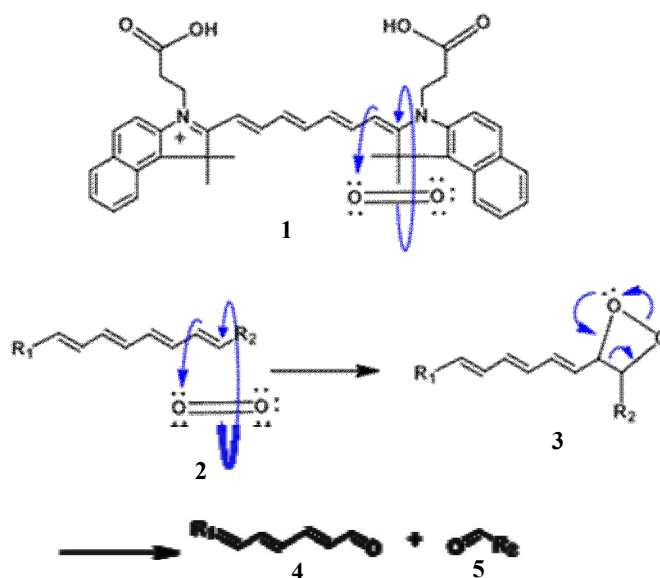


Figure 1: Mechanism of the photobleaching of Cypate by singlet oxygen. This illustrates the photobleaching that occurs *in vitro* and *in vivo* following absorbance of light in NIR region of the spectrum.

142

143

144

145

146

147

148

149

150

151

152

153

154

155

156

157

158

159

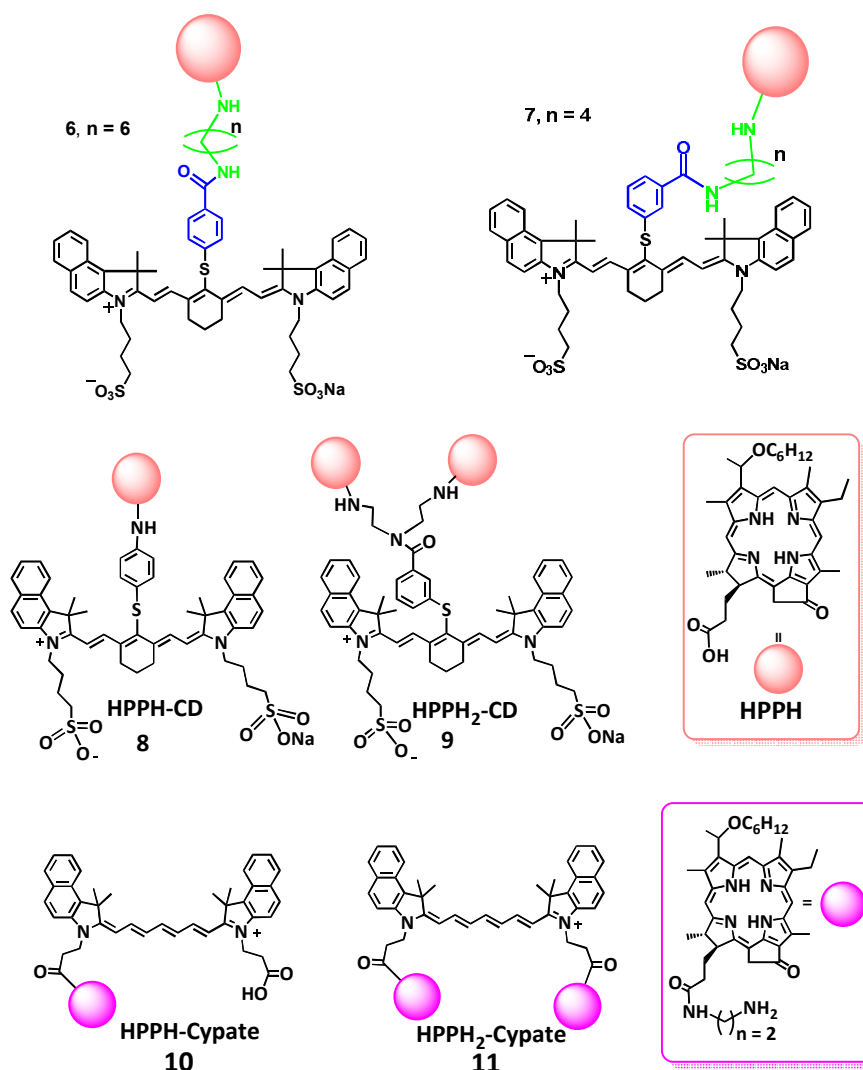


Figure 2: Structures of the conjugates 6-11 used for the study

160

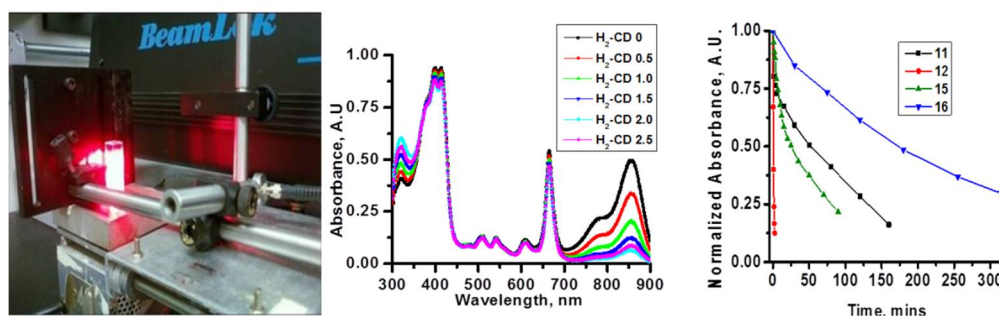


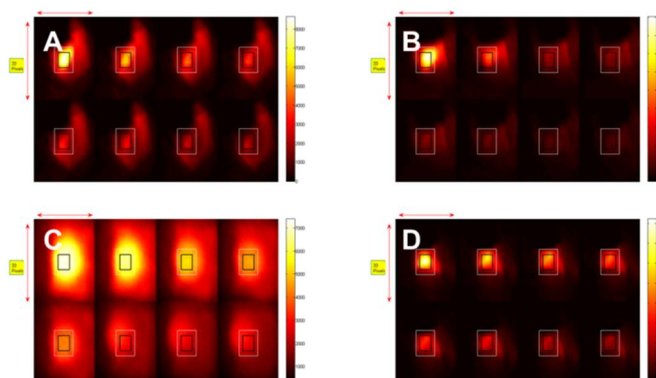
Figure 3: Photobleaching of the conjugates as 5 μ M solutions in 17% BCS in PBS. HPPH-CD (8), HPPH₂CD (9), HPPH-Cypate (10) and HPPH₂-Cypate (11) were photobleached *in vitro* in the order of 9 > 10 > 8 > 11.

2.3. *In Vivo* Photo-induced bleaching kinetics

BALB/c mice (3/group) were inoculated with compounds, 8, 9, 10 and 11 and monitored during PDT for 30 minutes at various time intervals. The tumors were irradiated at a wavelength 665 nm using a total light dose of 135 J/cm² and fluence rate of 75 mW/cm², respectively. Concurrently, the fluorescence kinetics were monitored by illuminating at 785 nm and measuring the fluorescence

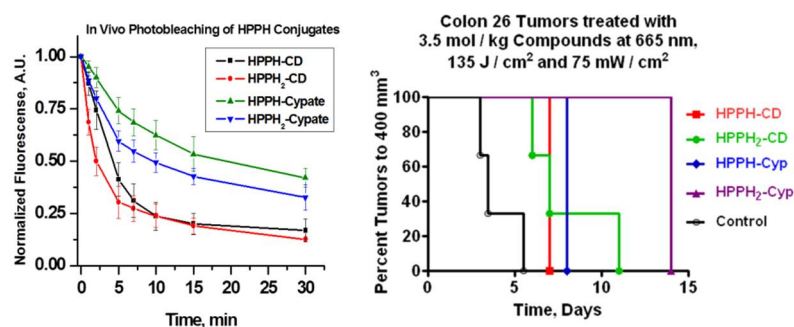
169 with a 830 long pass filter. Figure 3 shows images of the photo-induced bleaching kinetics of the four
 170 conjugates **8**, **9**, **10** and **11** at different time points during treatment. The mice injected with
 171 HPPH-Cypate (**10**) were irradiated at 661 nm. PDT efficacy of HPPH-CD (**8**), HPPH₂CD (**9**),
 172 HPPH-Cypate (**10**) and HPPH₂Cypate (**11**) was also assessed after the photo-induced bleaching
 173 experiment, as shown in Figure 4. We observed that there were no PDT cures upon assessment of the
 174 tumor response (**Figures 4 & 5**). All mice were sacrificed when the tumor sizes grew to a volume of
 175 400 mm³. The dismal tumor response could be due to changes in tumor oxygenation induced by
 176 high fluence rates [31]. High fluence rates such as that used in this experiment (135 J/cm² and 75
 177 mW/cm²) can cause the depletion of molecular oxygen during the process of singlet oxygen
 178 generation, which can exceed the rate at which it can be resupplied by diffusion from the vasculature
 179 [31].

180 **Figure 4:** Photobleaching of (A)
 181 HPPH-CD (**8**), (B) HPPH₂CD (**9**), (C)
 182 HPPH-Cypate (**10**) and (D)
 183 HPPH₂Cypate (**11**) All conjugates were
 184 irradiated at 665 nm, except in the case 15
 185 (661 nm) and treated at a fluence and
 186 fluence rate of 135 J/cm² and 75 mW/cm².
 187 Concurrently fluorescence images were
 188 taken at various treatment times up to 30
 189 minutes, the total treatment time



190

191 **Figure 5:** *In vivo* phot bleaching
 192 of the conjugates HPPH-CD (**8**),
 193 HPPH₂CD (**9**), HPPH-Cypate
 194 (**10**) and HPPH₂-Cypate (**11**)
 195 occurred in the order of 9 > 8 >
 196 11 > 10. There were no PDT
 197 cures upon assessment of the
 198 tumor response. All mice were
 199 sacrificed when they grew to a
 200 volume of 400 mm³.



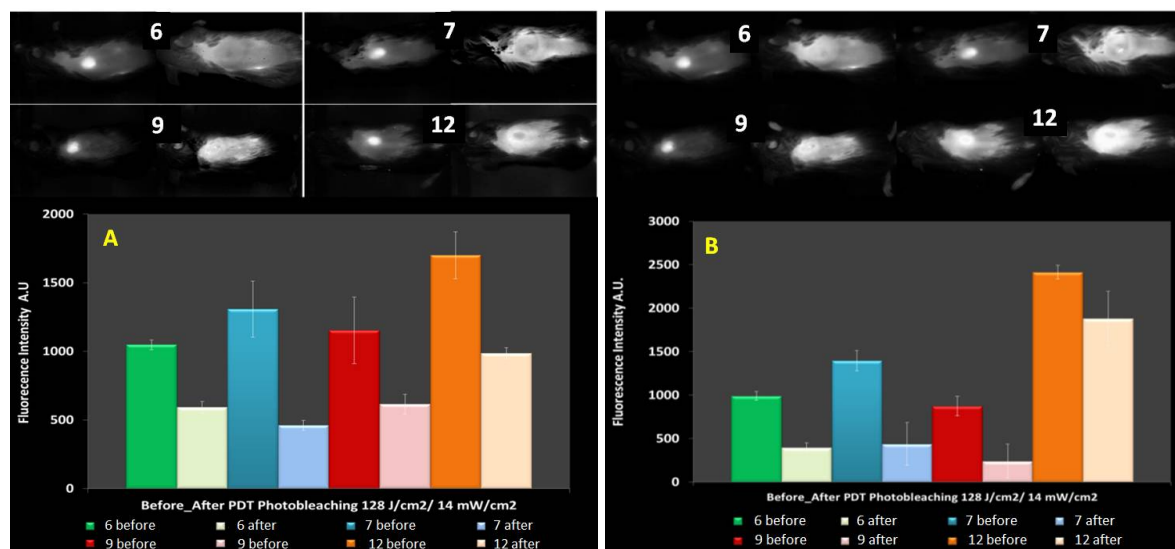
201

202 It is believed that such occurrences would lead to PDT self-limiting hypoxic conditions [31]
 203 whereby the tumor and surrounding regions becomes deprived of oxygen. Therefore we adapted
 204 the following experiments with the low-fluence rates.

205

206 2.4. *In Vivo* Photobleaching Before and After Low-fluence rate PDT Treatments

207 It has been demonstrated that there was a direct relationship between the tumor response and the
 208 level of oxygen within the tumor tissue during PDT [31-38]. Additionally, it has also been
 209 demonstrated that using HPPH as a PS and exposing the tumor at low light fluence and fluence
 210 rate of 128 J/cm² and 14 mW/cm² showed better tumor response rates with cures up 90 days after
 211 PDT [31,33]. Another observation made during these experiments was that the tumor response for
 212 the fluence of 128 J/cm² increased as the fluence rate decreased further [31,33]. Therefore, to
 213 understand the impact of these light treatment parameters in PDT efficacy of the PS-CD conjugates,
 214 the photobleaching experiments were conducted at various fluence and fluence rates of 135 J/cm²
 215 and 75 mW/cm²; 128 J/cm² and 14 mW/cm² and 128 J/cm² and 7 mW/cm²



216

217 **Figure 6:** (A) Photobleaching of the HPPH portion of PS-CD
 218 conjugates, and (B) a comparative photobleaching of the CD moiety
 219 in HPPH-CD conjugates 6, 7, 9 and 12 at the light dose of 128 J/cm²
 220 and 14 mW/cm²

221

222

223

224

225

226

227

228

229

In these experiments, the fluorescence was observed before and after PDT treatment at the fluence and fluence rates mentioned above. The compounds chosen for this study were conjugates 6, 7, 9 (Figure 2) and 12 (Figure 7) on the basis of their significant *in vitro* and *in vivo* PDT responses in mice bearing Colon-26 and U87 tumor models [29,30].

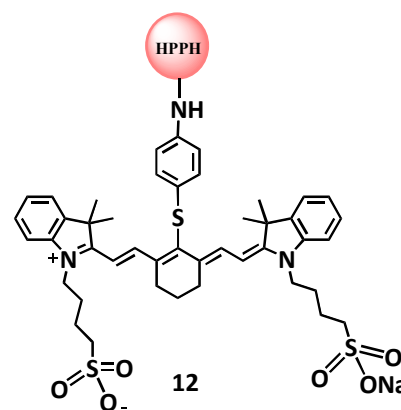


Figure 7: Structure of HPPH-CD conjugate 12

Compounds			Fluorescence				Photobleached 128 J/cm ² 14mW/cm ²		% Tumor Cured 128 J/cm ² 14mW/cm ²
Drug #	PS	Dose (umol /kg)	Pre PDT HPPH	Pre PDT CD	Post PDT HPPH	Post PDT CD	% PBLCH HPPH	% PBLCH CD	PDT ONLY
6	LLP	1.5	1048	989	592	397	43	60	80
7	MLM	1.5	1308	1396	460	439	65	69	80
9	H2CH	1.5	1154	874	616	239	47	73	80
12	H783NH2	1.5	1701	2413	986	1881	42	22	40

230

231

Table 1: Summary of *in vivo* photobleaching of HPPH moiety in HPPH-CD conjugates 6, 7, 9 and 12 at 128 J/cm² and 14 mW/cm²

232

233

234

The photobleaching data obtained from these experiments were used in conjunction with the molecular modeling of the compounds to infer possible optimization of PDT light dosimetry since it has been reported that it is not simple to predict the photobiological outcome from *in vivo*

235 photobleaching data alone, because of the complex dependence on oxygenation and
236 micro-environment factors [22].

237 The fluorescence intensities of HPPH and the CD were also compared prior to light irradiation and
238 at the end of treatment with light dose of 128 J/cm² and 14 mW/cm². After combining the data
239 obtained from the three mice in each group it was found that the HPPH (PS) portion of compounds
240 **6**, **7**, **9** and **12** photobleached by 43%, 65%, 47% and 42% respectively; whereas, the CD portion
241 underwent photobleaching by 60%, 69%, 73%, and 22% respectively.

Compounds			Fluorescence				Photobleached 48 J/cm ² 7mW/cm ²		% Tumor Cured 48 J/cm ² 7mW/cm ²
Dru g#	PS	Dose (μ mol/ kg)	Pre PDT HPPH	Pre PDT CD	Post PDT HPPH	Post PDT CD	% PBLCH HPPH	% PBLH CD	PDT ONLY
6	LLP	1.5	1060	976	825	492	22	50	ND
7	MLM	1.5	1485	1319	1170	1019	21	23	ND
9	H2CH	1.5	986	809	808	459	18	43	ND
12	H783NH2	1.5	1428	2538	1238	1783	13	30	ND

242 **Table 2:** Summary of the photobleaching results with conjugates **6**, **7**, **9** and **12** at a light dose of 48 J/cm² and
243 7mW/cm². The PDT activity of the conjugates at a light dose of 48J/cm², 7mW/cm² was not determined (ND).

244 Under similar treatment parameters, the photobleaching rates of the CD portion of the conjugate in
245 **6**, **7**, and **9** were observed in the range of 60 – 73% when irradiated at 128 J/cm² and 14mW/cm²
246 On the other hand, the PDT response was 40% for conjugate **9** with only 20% photobleaching
247 observed for the CD (**Table 1**). These results suggest that there is a direct correlation between the
248 rate of photobleaching of the CD and the tumor response; more the photobleaching of the CD in
249 HPPH-CD conjugates, the higher was the tumor response. It was difficult to infer a similar
250 conclusion in the case of HPPH photobleaching with respect to tumor response, since the
251 photobleaching rates were quite similar for all the cases except compound **6**. Summary of
252 photobleaching rates of **6**, **7**, **9** and **12** at 128 J/cm² and 14 mW/cm² are shown in Tables 1 & 2.

253 There was no PDT response when a fluence and fluence rate of 128 J/cm² and 7 mW/cm² was used.
254 This can be explained by the threshold dose beyond which the repair of sub-lethal damage
255 overrides the advantages of low fluence rate [31,39,40]. However, in the experiment where fluence
256 rates of 135 J/cm² and 75mW/cm² (**Table 2**) were used, the photo-induced bleaching of the CD
257 portion of the conjugate was between 16% and 52%, and there was a tumor response of 66% and
258 33% for compounds **9** and **12**, respectively. The degree of photobleaching of the HPPH moiety also
259 correlated well with the NIRF moiety. Therefore, the less photobleached the HPPH or NIRF at 135
260 J/cm² and 75 mW/cm² the better was the response. This could also be due to with the amount
261 accumulated conjugate (PS) within the tumor before PDT light illumination. It has been shown that
262 the combination of fluence and fluence rate can lead to anoxic conditions within the first few
263 minutes of illumination [31,33]. Therefore, it can be deduced that if the amount of photosensitizer
264 accumulated within the tumor prior to PDT is high this would help to circumvent the observance
265 of anoxic conditions

Compounds			Fluorescence				Photobleached 135 J/cm ² 75mW/cm ²		% Tumor Cured 135 J/cm ² 75mW/cm ²	
Drug #	PS	Dose (umol/kg)	Pre PDT HPPH	Pre PDT CD	Post PDT HPPH	Post PDT CD	% PBLCH HPPH	% PBLCH CD	% Tumor cure	
6	LLP	1.5	1136	1025	670	416	41	60	0	
7	MLM	1.5	1380	1319	655	560	53	58	0	
9	H2CH	1.5	996	904	683	430	31	52	33	
12	H783NH2	1.5	1392	2543	1390	2143	8	16	66	

266 **Table 3:** Summary of the photobleaching of conjugates **6**, **7**, **9** and **12** at 135 J/cm² and 75 mW/cm²

267 3. Conclusion

268 The data acquired from the *in vitro* photo-induced bleaching of conjugates showed that NIR
 269 fluorophore CD of the conjugates photobleached at a much faster rate than HPPH and the rate of
 270 bleaching was in the order of **9** > **10** > **8** > **11**, which correlated well with their *in vivo* PDT responses
 271 when irradiated at 128 J/cm² and 14 mW/cm², using a drug dose of 1.5 umol/kg. Conjugate **12**
 272 produced 80% tumor response, whereas compounds **10** and **11** did not yield any long-term cure.
 273 The *in vivo* photobleaching of HPPH and CD in conjugates before and after PDT suggests that
 274 measuring the rate of the photobleaching of CD could be a useful tool to optimize the PDT light
 275 dosimetry. We hypothesize that the determining the rate of photobleaching of CD in PS-CD
 276 conjugates may help to measure indirectly the amount of singlet oxygen generation during
 277 photodynamic therapy treatment at variable light fluence and fluence rates [1, 22]. These studies
 278 are currently underway.

279 According to Wilson et al the use of photobleaching as a dose metric is based on the fact that the
 280 photosensitizer or NIR fluorophore will be degraded directly or indirectly by singlet oxygen as it
 281 goes through each photo-activation cycle [41]. An enhanced level of photo-activation is directly
 282 proportional to enhanced photobleaching. As a result, a hypothesis is proposed that greater
 283 photobleaching represents greater singlet oxygen production and hence an enhanced
 284 photodynamic efficacy [41]. However, this assumption/hypothesis may lead to several issues
 285 such as: (i) If the fluorescence of the PS is used for the measurements without knowing the absolute
 286 initial concentration of the PS, it could be difficult to determine the absolute number of PS
 287 molecules photobleached per unit volume during PDT [39]. It has been shown, however, that this
 288 requirement can be fulfilled by quantitative fluorescence imaging methods that can quantify
 289 absolute PS concentrations (ii) Molecular changes of the PS within tissue may result in changes to
 290 the fluorescence without any changes in PDT response [41]; (iii) Photobleaching rate itself may not
 291 be a sole indicator for PDT dosimetry/response [41], since it has been shown that singlet oxygen
 292 generation is dependent on the tissue microenvironment [4, 41]. The micro/local-distribution of the
 293 PS will be difficult to quantify because noninvasive or noninvasive fluorescence measurements are
 294 limited, and can only provide a measure of average/bulk value of the PS concentration.

295 Author Contributions:

296 Nadine James: Synthesis of the conjugates and biological evaluation (in vitro, in vivo) evaluation of the
 297 compounds. Nadine also prepared the first draft of the manuscript. Ravindra R. Cheruku: Synthesized some of

298 the PS-CD conjugates required to confirm the photophysical properties. Joseph Missert: Isolated the starting
299 material from *Spirulina pacifica*, which mainly contains chlorophyll-a. Ulas Sunar: Designed the *in vivo*
300 photobleaching experiments, helped in analyzing the data and also providing helpful comments on the
301 manuscript. Ravindra K Pandey: Overall supervision of the project including the design of the conjugates
302 studied in this project, providing financial assistance from the NIH funded grant in which he is the PI, and
303 refining the manuscript before submission.

304 **Acknowledgments**: The authors are thankful to NIH for the financial support: RO1 CA127369 (RKP), and
305 research supplement to promote diversity in health-related research to Nadine S. James (CA127369S). This
306 work utilized core resources supported by the NCI Cancer Center Support Grant CA016156 (Johnson: PI).

307 **Conflicts of Interest**: The authors declare no conflict of interest.

308 References

- 309 1. Jarvi Mark, T., Niedre Mark, J., Patterson Michael, S. & Wilson Brian, C. Singlet oxygen luminescence
310 dosimetry (SOLD) for photodynamic therapy: current status, challenges and future prospects. *Photochem*
311 *Photobiol* **2006**, *82*, 1198-1210.
- 312 2. Wilson, Brian C. & Patterson, Michael S. The physics, biophysics and technology of photodynamic
313 therapy. *Physics in Medicine & Biology* **2008**, *53*, R61-R109.
- 314 3. Fien, Sari M. & Oseroff, Allan R. Photodynamic therapy for non-melanoma skin cancer. *J. Natl. Compr.*
315 *Cancer Network* **2007**, *5*, 531-540.
- 316 4. Biel, M. A. Photodynamic therapy and the treatment of head and neck cancers. *Journal of clinical laser*
317 *medicine & surgery* **1996**, *14*, 239-244.
- 318 5. Friedberg, Joseph S., Mick, Rosemarie, Stevenson, James P., Zhu, Timothy, Busch, Theresa M., Shin,
319 Daniel, Smith, Debbie, Culligan, Melissa, Dimofte, Andreea, Glatstein, Eli & Hahn, Stephen M. Phase II
320 trial of pleural photodynamic therapy and surgery for patients with non-small-cell lung cancer with
321 pleural spread. *J. Clin. Oncol.* **2004**, *22*, 2192-2201.
- 322 6. Grant, W. E., Speight, P. M., Hopper, C. & Bown, S. G. Photodynamic therapy: an effective, but
323 non-selective treatment for superficial cancers of the oral cavity. *International journal of cancer. Journal*
324 *international du cancer* **1997**, *71*, 937-942.
- 325 7. Ackroyd, R., Brown, N. J., Davis, M. F., Stephenson, T. J., Marcus, S. L., Stoddard, C. J., Johnson, A. G. &
326 Reed, M. W. R. Photodynamic therapy for dysplastic Barrett's esophagus: A prospective, double blind,
327 randomized, placebo controlled trial. *Gut* **2000**, *47*, 612-617.
- 328 8. Overholt, B. F. & Panjehpour, M. Photodynamic therapy for Barrett's esophagus: clinical update. *Am J*
329 *Gastroenterol* **1996**, *91*, 1719-1723.
- 330 9. Overholt, B. F., Panjehpour, M. & Ayres, M. Photodynamic therapy for Barrett's esophagus: cardiac
331 effects. *Lasers Surg Med* **1997**, *21*, 317-320.
- 332 10. Overholt, B. F., Panjehpour, M. & Haydek, J. M. Photodynamic therapy for Barrett's esophagus: follow-up
333 in 100 patients. *Gastrointestinal endoscopy* **1999**, *49*, 1-7.
- 334 11. Overholt, Bergein F., Wang, Kenneth K., Burdick, J. Steven, Lightdale, Charles J., Kimmey, Michael, Nava,
335 Hector R., Sivak, Michael V., Jr., Nishioka, Norman, Barr, Hugh, Marcon, Norman, Pedrosa, Marcos,
336 Bronner, Mary P., Grace, Michael & Depot, Michelle. Five-year efficacy and safety of photodynamic
337 therapy with Photofrin in Barrett's high-grade dysplasia. *Gastrointestinal endoscopy* **2007**, *66*, 460-468.
- 338 12. Biel, M. Advances in photodynamic therapy for the treatment of head and neck cancers. *Lasers Surg Med*
339 **2006**, *38*, 349-355.
- 340 13. Bogaards, Arjen, Varma, Abhay, Zhang, Kai, Zach, David, Bisland, Stuart K., Moriyama, Eduardo H.,
341 Lilge, Lothar, Muller, Paul J. & Wilson, Brian C. Fluorescence image-guided brain tumor resection with
342 adjuvant metronomic photodynamic therapy: pre-clinical model and technology development. *Photochem.*
343 *Photobiol. Sci.* **2005**, *4*, 438-442.
- 344 14. Rosenthal, Mark A., Kavar, Bhadu, Hill, John S., Morgan, Denis J., Nation, Roger L., Stylli, Stanley S.,
345 Basser, Russell L., Uren, Shannon, Geldard, Howard, Green, Michael D., Kahl, Stephen B. & Kaye, Andrew
346 H. Phase I and pharmacokinetic study of photodynamic therapy for high-grade gliomas using a novel
347 boronated porphyrin. *J. Clin. Oncol.* **2001**, *19*, 519-524.
- 348 15. Stylli, Stanley S., Howes, Megan, MacGregor, Lachlan, Rajendra, Priya & Kaye, Andrew H. Photodynamic
349 therapy of brain tumours: evaluation of porphyrin uptake versus clinical outcome. *J. Clin. Neurosci.* **2004**,
350 *11*, 584-596.

- 351 16 Stylli, Stanley S. & Kaye, Andrew H. Photodynamic therapy of cerebral glioma - A review Part I - A
352 biological basis. *J. Clin. Neurosci.* **2006**, *13*, 615-625.
- 353 17 Stylli, Stanley S., Kaye, Andrew H., MacGregor, Lachlan, Howes, Megan & Rajendra, Priya.
354 Photodynamic therapy of high grade glioma - long term survival. *J. Clin. Neurosci.* **2005**, *12*, 389-398.
- 355 18 Stripp, Diana C. H., Mick, Rosemarie, Zhu, Timothy C., Whittington, Richard, Smith, Debbie, Dimofte,
356 Andreea, Finlay, Jarod C., Miles, Jeremy, Busch, Theresa M., Shin, Daniel, Kachur, Alex, Tochner, Zelig A.,
357 Malkowicz, S. Bruce, Glatstein, Eli & Hahn, Stephen M. Phase I trial of motexafin-lutetium-mediated
358 interstitial photodynamic therapy in patients with locally recurrent prostate cancer. *Proc. SPIE-Int. Soc.*
359 *Opt. Eng.* **2004**, *5315*, 88-99.
- 360 19 Weersink, Robert A., Wilson, Brian C., Bogaards, Arjen, Gertner, Mark R., Davidson, Sean R. H., Haider,
361 Masoom A., Elhilali, Mostafa & Trachtenberg, John. Vascular-targeted photodynamic of prostate cancer
362 phase with Tookad for recurrent prostate cancer following radiation therapy: Initial clinical studies. *Proc.*
363 *SPIE-Int. Soc. Opt. Eng.* **2007**, *6424*, 64241E/64241-64241E/64210.
- 364 20 Weersink Robert, A., Bogaards, Arjen, Gertner, Mark, Davidson Sean, R. H., Zhang, Kai, Netchev, George,
365 Trachtenberg, John & Wilson Brian, C. Techniques for delivery and monitoring of TOOKAD
366 (WST09)-mediated photodynamic therapy of the prostate: clinical experience and practicalities. *Journal of*
367 *photochemistry and photobiology. B, Biology* **2005**, *79*, 211-222.
- 368 21 Miyagi, Kiyoko, Sampson, Reynee W., Sieber-Blum, Maya & Sieber, Fritz. Crystal violet combined with
369 Merocyanine 540 for the ex vivo purging of hematopoietic stem cell grafts. *Journal of Photochemistry and*
370 *Photobiology, B: Biology* **2003**, *70*, 133-144.
- 371 22 McIlroy, Brian W., Mann, Thomas S., Dysart, Jonathan S. & Wilson, Brian C. The effects of oxygenation
372 and photosensitizer substrate binding on the use of fluorescence photobleaching as a dose metric for
373 photodynamic therapy. *Vibrational Spectroscopy* **2002**, *28*, 25-35.
- 374 23 Ascencio, Manuel, Collinet, Pierre, Farine, M. O. & Mordon, Serge. Protoporphyrin IX fluorescence
375 photobleaching is a useful tool to predict the response of rat ovarian cancer following hexaminolevulinate
376 photodynamic therapy. *Lasers Surg Med* **2008**, *40*, 332-341.
- 377 24 McIlroy, Brian W., Mann, Thomas S., Dysart, Jonathan S. & Wilson, Brian C. The effects of oxygenation
378 and photosensitizer substrate binding on the use of fluorescence photobleaching as a dose metric for
379 photodynamic therapy. *Vibrational Spectroscopy* **2002**, *28*, 25-35.
- 380 25 Wilson, B. C., Patterson, M. S. & Lilge, L. Implicit and explicit dosimetry in photodynamic therapy: a New
381 paradigm. *Lasers Med Sci* **1997**, *12*, 182-199.
- 382 26 Zhu, Timothy C. & Finlay, Jarod C. The role of photodynamic therapy (PDT) physics. *Med. Phys.* **2008**, *35*,
383 3127-3136.
- 384 27 Patterson, Michael S., Madsen, Steen J. & Wilson, Brian C. Experimental tests of the feasibility of singlet
385 oxygen luminescence monitoring in vivo during photodynamic therapy. *Journal of Photochemistry and*
386 *Photobiology, B: Biology* **1990**, *5*, 69-84.
- 387 28 Streckowski, Lucjan & Editor. Heterocyclic Polymethine Dyes; Synthesis, Properties and Applications. [In:
388 *Top. Heterocycl. Chem.*, **2008**; 14]. (Springer GmbH, **2008**).
- 389 29. James. Nadine S., Chen, Yihui, Joshi, Penny., Ohulchanskyy, Tymish Y., Ethirajan, M., Henary, M.,
390 Streckowsk, L. and Pandey Ravindra K. Evaluation of polymethine dyes as potential probes for near
391 infrared fluorescence imaging of tumors: Part-I. *Theranostics*, **2013**, *3*, 692-702.
- 392 30. James. Nadine S., Ohulchanskyy, Tymish Y Chen, Y., Joshi, Penny, Zheng, Xiang, Goswami, Lalit N. and
393 Pandey Ravindra K. Comparative tumor imaging and PDT efficacy of HPPHconjugated in the mono- and
394 di-forms to various polymethine cyanine dyes: Part-2. *Theranostics*, **2013**, *3*, 703-718.
- 395 31 Henderson, Barbara W., Busch, Theresa M. & Snyder, John W. Fluence rate as a modulator of PDT
396 mechanisms. *Lasers Surg Med* **2006**, *38*, 489-493.
- 397 32 Achilefu, Samuel, Bornhop, Darryl J., Raghavachari, Ramesh & Editors. Molecular Probes for Biomedical
398 Applications II. (Proceedings held in San Jose, CA 21-22 January **2008**). [In: *Proc. SPIE*, **2008**; 6867]
- 399 33 Henderson, Barbara W., Gollnick, Sandra O., Snyder, John W., Busch, Theresa M., Kousis, Philaretos C.,
400 Cheney, Richard T. & Morgan, Janet. Choice of Oxygen-Conserving Treatment Regimen Determines the
401 Inflammatory Response and Outcome of Photodynamic Therapy of Tumors. *Cancer Res.* **2004**, *64*,
402 2120-2126.

- 403 34 Pogue, Brian W., Sheng, Chao, Benevides, Juan, Forcione, David, Puricelli, Bill, Nishioka, Norm & Hasan,
404 Tayyaba. Protoporphyrin IX fluorescence photobleaching increases with the use of fractionated irradiation
405 in the esophagus. *Journal of biomedical optics* **2008**, *13*, 034009/034001-034009/034010.
- 406 35 Robinson, Dominic J., De, Bruijn Henriette S., Van, Der Veen Nynke, Stringer, Mark R., Brown, Stanley B.
407 & Star, Willem M. Fluorescence photobleaching of ALA-induced protoporphyrin IX during photodynamic
408 therapy of normal hairless mouse skin: the effect of light dose and irradiance and the resulting biological
409 effect. *Photochem. Photobiol.* **1998**, *67*, 140-149.
- 410 36 Robinson, Dominic J., De, Bruijn Henriette S., Van, Der Veen Nynke, Stringer, Mark R., Brown, Stanley B.
411 & Star, Willem M. Protoporphyrin IX fluorescence photobleaching during ALA-mediated photodynamic
412 therapy of UVB-induced tumors in hairless mouse skin. *Photochem. Photobiol.* **1999**, *69*, 61-70.
- 413 37 Sheng, Chao, Hoopes, P. Jack, Hasan, Tayyaba & Pogue, Brian W. Photobleaching-based dosimetry
414 predicts deposited dose in ALA-PpIX PDT of rodent esophagus. *Photochem. Photobiol.* **2007**, *83*, 738-748.
- 415 38 van, Veen Robert L. P., Aalders, Maurice C. G., Pasma, Kasper L., Siersema, Peter D., Haringsma, Jelle,
416 van, de Vrie Wim, Gabeler, Edward E. E., Robinson, Dominic J. & Sterenborg, Henricus J. C. M. In situ
417 light dosimetry during photodynamic therapy of Barrett's esophagus with 5-aminolevulinic acid. *Lasers*
418 *Surg Med* **2002**, *31*, 299-304.
- 419 39 Patterson, Michael S. & Wilson, Brian C. A theoretical study of the influence of sensitizer photobleaching
420 on depth of necrosis in photodynamic therapy. *Proc. SPIE-Int. Soc. Opt. Eng.* **1994**, *2133*, 208-219.
- 421 40 Patterson, Michael S., Wilson, Brian C. & Graff, Ronald. In vivo tests of the concept of photodynamic
422 threshold dose in normal rat liver photosensitized by aluminum chlorosulfonated phthalocyanine.
423 *Photochem. Photobiol.* **1990**, *51*, 343-349.
- 424 41 Wilson, Brian C., Weersink, Robert A. & Lilge, Lothar. 529-561 (Marcel Dekker, Inc.).